Retrieving Soil Moisture from Sentinel-1: Limitations over Certain Crops and Sensitivity to the First Soil Thin Layer

Hassan Bazzi, Nicolas Baghdadi, Pasquale Nino, Rosario Napoli, Sami Najem, Mehrez Zribi, Emmanuelle Vaudour

water

MDPI

Article

Retrieving Soil Moisture from Sentinel-1: Limitations over Certain Crops and Sensitivity to the First Soil Thin Layer

Hassan Bazzi [1,2,*], Nicolas Baghdadi [3], Pasquale Nino [4], Rosario Napoli [5], Sami Najem [3], Mehrez Zribi [6] and Emmanuelle Vaudour [7]

1 Université Paris-Saclay, AgroParisTech, INRAE, UMR 518 MIA Paris-Saclay, 91120 Palaiseau, France
2 Atos France, Technical Services, 95870 Bezons, France
3 TETIS, Université de Montpellier, CIRAD/CNRS/INRAE, 34093 Montpellier, France
4 CREA Research Centre for Agricultural Policies and Bioeconomy (CREA-PB), 06121 Perugia, Italy; pasquale.nino@crea.gov.it
5 CREA Research Centre for Agriculture and Environment (CREA-AA), 00184 Rome, Italy; rosario.napoli@crea.gov.it
6 CESBIO (CNES/CNRS/INRAE/IRD/UT3-Paul Sabatier), 31400 Toulouse, France; mehrez.zribi@ird.fr
7 Université Paris-Saclay, AgroParisTech, INRAE, UMR EcoSys, 91120 Palaiseau, France; emmanuelle.vaudour@inrae.fr
* Correspondence: hassan.bazzi@agroparistech.fr

Abstract: This paper presents a comparison between the Sentinel-1 (S1)/Sentinel-2 (S2)-derived soil moisture products at plot scale (S^2MP) and in situ soil moisture measurements at a 10 cm depth for several winter and summer crops. Specifically, the paper discusses the consistency between the in situ soil moisture measurements, usually performed at a 10 cm soil depth, and the variable S1 C-band penetration depth in soil due to soil humidity conditions, vegetation development and S1 acquisition configuration. The aim is to provide end users with the strength and limitations of S1-derived soil moisture, mainly the S^2MP soil moisture product, for their further applications. Both the estimated and measured soil moisture (SM) were evaluated over three testing fields in a Mediterranean climatic context, with crop cycles including wheat, tomato, cover crops and soybeans. The main results showed that the comparison between the S^2MP-estimated SM based on S1 backscattering (at ~5 cm depth) with a 10 cm in situ SM is not always relevant during the crop cycle. In dry conditions, the S1 SM significantly underestimated the 10 cm SM measurements with an underestimation that could reach around 20 vol.% in some extremely dry conditions. This high underestimation was mainly due to the difference between the topsoil SM captured by the S1 sensor and the 10 cm in depth SM. Moderately wet conditions due to rainfall or irrigation showed less of a difference between the S1-estimated SM and the 10 cm in situ SM and varying between −10 and −5 vol.% due to the homogeneity of the SM at different soil depths. For extremely wet conditions, the S1 SM started to underestimate the SM values with an underestimation that can reach an order of −10 vol.%. A comparison of the S1-estimated SM as a function of the vegetation development showed that, for the studied crop types, the S1 SM estimates are only valid for low and moderate vegetation cover with a Normalized Difference Vegetation Index (NDVI) of less than 0.7. For dense vegetation cover (NDVI > 0.7), overestimations of the SM (average bias of about 4 vol.%) are mainly observed for developed tomato and soybean crops due to fruits' emergence, whereas an extreme underestimation (average bias reaching −15.5 vol.%) is found for developed wheat cover due to the vertical structure of the wheat kernels. The results also suggest that the optimal SM estimations by S1 could be mainly obtained at low radar incidence angles (incidence angle less than 35°).

Keywords: S^2MP; topsoil moisture; agricultural areas; penetration depth; vegetation cover

Citation: Bazzi, H.; Baghdadi, N.; Nino, P.; Napoli, R.; Najem, S.; Zribi, M.; Vaudour, E. Retrieving Soil Moisture from Sentinel-1: Limitations over Certain Crops and Sensitivity to the First Soil Thin Layer. *Water* **2024**, *16*, 40. https://doi.org/10.3390/w16010040

Academic Editor: Maria Mimikou

Received: 18 October 2023
Revised: 4 December 2023
Accepted: 19 December 2023
Published: 21 December 2023

1. Introduction

Soil moisture (SM) plays a major role in several applications, including hydrology, agronomy and environmental risk management [1,2]. Currently, space remote sensing observations provide operational tools for mapping the spatial and temporal variations in SM over wide areas [3–8], which is considered essential for land–water management strategies, especially in croplands. Over the last decade, several operational approaches were developed using Synthetic Aperture Radar (SAR) data for SM mapping, either on a field scale or on a medium scale [4,9–11]. Recently proposed approaches mainly focused on the use of Sentinel-1 SAR sensors (S1) developed by the European Space Agency (ESA) that provide open-source, free-of-charge and multitemporal C-band SAR images with a high revisit time (6 days) and a pixel spacing of 10 m. The C-band SAR sensor, with a wavelength of ~5 cm, is expected to provide the soil moisture estimation of the cultivated soil's topmost 5 cm layer. Several SM products using the S1 C-band satellite observations are operational and available for end users, including, but not limited to, the Copernicus Surface SM product (CSSM) at a 1 km grid scale [3], the joint SMAP (Soil Moisture Active Passive) S1 product at a 3 km grid scale [12] and the Sentinel-1/Sentinel-2-derived Soil Moisture Product (S^2MP).

To provide users with a robust evaluation of the soil moisture estimation accuracies, several studies compared S1-derived soil moisture products with in situ measured soil moisture and intercompared between different SM products [13–15]. Such studies usually report the soil moisture accuracy using common evaluation metrics such as the correlation coefficient (R), the Root Mean Squared Error (RMSE) and the bias between measured and in situ soil moisture. Although this general evaluation using common statistical metrics could present the overall estimation accuracy, it could be sometimes misleading if not deeply examined with other factors that could affect both the SM estimation and the SM in situ measurements. Indeed, few detailed evaluations of the S1 SM retrieval limitations regarding the radar sensitivity to soil depth, the performed in situ soil moisture depth and the vegetation cover (density, crop type, phenological stage, etc.) have been presented. First, one of the main issues when comparing an S1-derived soil moisture product with the in situ measurements is the penetration mismatch between the C-band SAR measurements and the in situ measurements. Conventionally, during field campaigns, in situ soil moisture measurements are generally performed at a 10 cm depth for all fields along a vegetation cycle, using the Time Delay Reflectometer (TDR) or meteorological networks [16]. On the other hand, the penetration of the S1 C-band signal (wavelength, ~5 cm) in the soil layer could be difficult to quantify. In fact, the exact penetration of the S1 C-band signal (from surface to 5 cm) depends on the dielectric constant of the soil and therefore on both the soil moisture and the soil composition (soil texture, soil density), thus making the C-band penetration depth variable between one plot and another, as well as for the same plot at different periods of the year [17]. Second, the vegetation cover could also be another limitation for the penetration depth of the S1 signal. In fact, the ability of the S1 signal to penetrate the canopy cover varies with the crop type, the crop development and the crop density. In this context, some studies showed that the S1 SM estimations are limited for low-to-moderately developed canopy cover, thus making the use of S1 SM estimations penalizing since retrieving the SM under well-developed vegetation cover is fundamental for crop vegetation monitoring and irrigation management. For example, El Hajj et al. [18] reported that the C-band SAR signal has no sensitivity to SM for wheat canopies with an NDVI (Normalized Difference Vegetation Index) exceeding 0.7. Gao et al. [19] showed that the SM estimation accuracy decreases as the NDVI increases and that the SM estimation accuracy reached 9 vol.% for an NDVI of 0.8. Nevertheless, the limitations in the penetration of the S1 signal to crop cover have not yet been extensively explored for several crop types, thus making it difficult to determine during which period of the crop cycle and for which crop type (or crop family) the S1-estimated SM remains relevant.

Given the aforementioned limitations of the S1 SAR data to retrieve SM estimates, it is of great importance for end users to understand the reliability of the S1 SM estimates and be

aware of the S1 SM retrieval accuracy. With S1 SM products being operationally available for users, assessing these limitations can help identify where and when to use these kinds of SM estimates in further agronomical, hydrological or environmental applications. Therefore, the objective of this paper is to provide a deeper and detailed assessment of the strengths and limitations of the S1 soil moisture estimations at the plot scale from the S^2MP, focusing on three main points:

1. The consistency between the S1-estimated soil moisture by S^2MP and the conventional soil moisture measurements made at a 10 cm depth along a crop cycle/year.
2. The limitation of the S1 SM estimations for developed vegetation cover, considering common winter crops and summer irrigated crops (wheat, soybean, tomato and cover crops).
3. Evaluate the effect of the S1 acquisition configuration (S1 incidence angle) on the S1 SM estimations.

2. Materials and Methods

2.1. Study Sites

Two different test sites were considered in this study, one located in Central Italy, Lazio Region, called IT-LAZ, with two experimental fields; and the other in the North Est Italy, Veneto Region, called IT-VE, with one experimental field (Figure 1). We selected the two sites based on the availability of long-term SM measurements to analyze Sentinel 1-derived SM for various crops and crop development stages.

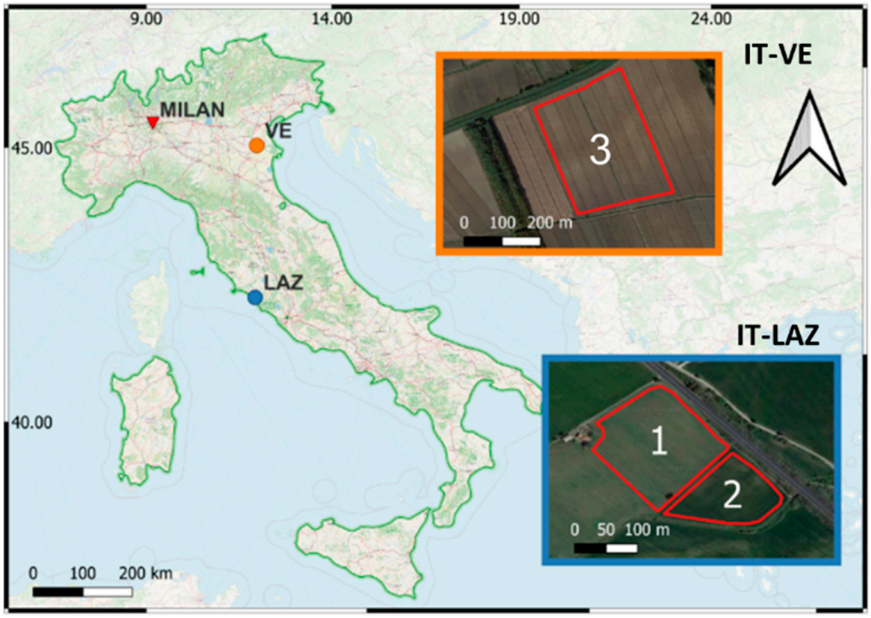

Figure 1. Study sites and experimental fields' locations (red polygon).

2.1.1. IT-LAZ

The test site IT-LAZ is situated in an agricultural area north of Rome within the Tarquinia municipality of Central Italy (study site central coordinates 42°23′ N, 12°16′ E, 25 m a.s.l., Datum WGS84), approximately 3 km from seashore. The predominant land use is intensive agriculture, characterized by rainfed winter cereals and irrigated summer horticultural crops. Figure 2 shows the experimental plots at the IT-LAZ site (Figure 2a), along with the crop calendar spanning from 2015 to 2017 (Figure 2b).

The climate is typically Mediterranean, characterized by warm, dry summers, mild winters and an average annual rainfall of approximately 600 mm, mainly concentrated in autumn and spring. The mean daily temperature is 15 °C (ranging from 7 °C in January to 23 °C in July). According to the World Reference Base for soil resources (WRB 2014),

field 1's soil is classified as Haplic Phaeozems developed on Quaternary Marine terraces on rolling and gently undulated slopes, with a dominant topsoil with a fine–loamy texture. Field 2 is classified as Haplic Phaeozems colluvial situated in flat alluvial valleys inside marine terraces, with a dominant topsoil of a loamy texture. The field experiment started in autumn 2015, covering a total area of about 3 ha. The area is conventionally cultivated with rotations of durum wheat (*Triticum durum* of Iride variety), cover crops (*Vicia faba* of minor Beck variety) and processing tomato (*Solanum lycopersicum* L. variety Vulcano), as depicted in Figure 2a,b.

(**a**)

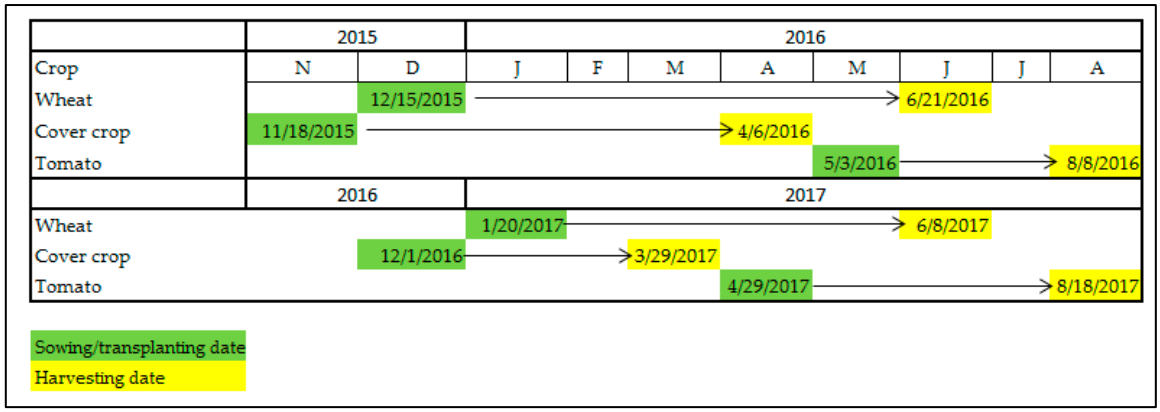

(**b**)

Figure 2. (**a**) Location of the experimental IT-LAZ plots used in this study (plots 1 and 2). Red dot represents the soil moisture measurement points at a 10 cm depth and (**b**) crop calendar for IT-LAZ plots from 2015 to 2017.

- in situ SM data at 10 cm

Soil Moisture was recorded through a profile probe PR 2/6 (Frequency Domain Reflectometry), giving readings at 10/20/30/40/60 and 100 cm, with a half-hour frequency (https://www.delta-t.co.uk/product/pr2/ (accessed on 12 December 2023)) (Figure 2a). For this study's purposes, only SM records at 10 cm in depth were considered. A detailed description of the experimental setup is given by Vanino et al. [20]. The periods with SM measurements available for the analysis are outlined in Table 1.

Table 1. SM measurements available for the different crops and growing season.

	2015/2016		2017	
Crop	**From**	**To**	**From**	**To**
Wheat	4-February-16	16-June-16	11-January-17	5-June-17
Cover crop	10-November-15	5-April-16	11-January-17	29-March-17
Tomato	5-May-16	1-August-16	8-June-17	2-August-17

- Temperature and precipitation data

To describe the weather trend, daily meteorological data were obtained from the Agrometeorological Service Station of the Lazio Region (ARSIAL) situated in the Tarquinia Municipality, approximately 4 km eastward from the central point of the study area (Figure 3). The primary feature of the meteorological trend during the 2015–2016 and 2016–2017 seasons concerned the distribution of rainfall. Abundant rainfall during autumn delayed the sowing of wheat from the typical planting period in the 1st and 2nd decade from each November to December–January. December and January were generally cold and dry; subsequently, rainfall resumed from late January to mid-February, displaying different trends during the two growing seasons between 2016 and 2017. The 2015–2016 growing season experienced higher rainfall, accumulating 257 mm between January and June of 2016, compared to 64.5 mm in the 2016–2017 growing season for the same period.

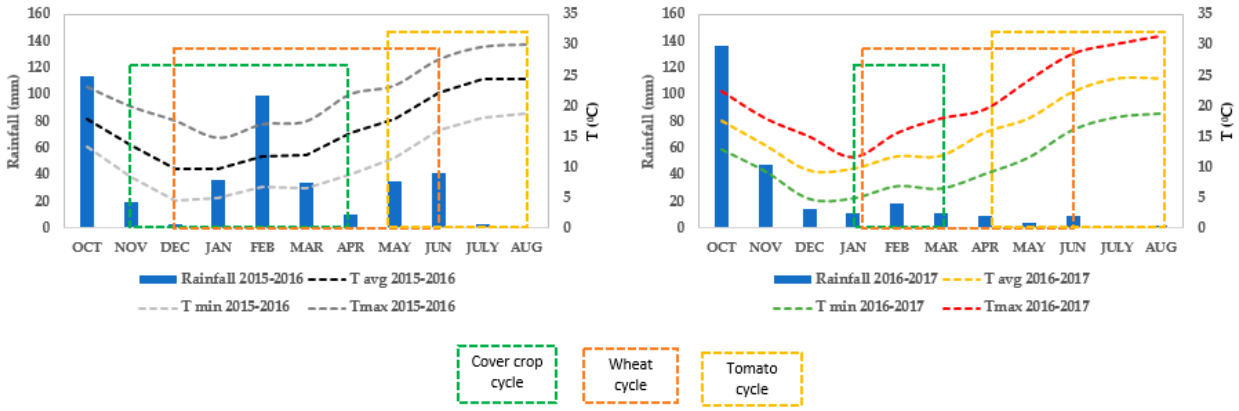

Figure 3. Monthly rainfall (mm) with average, minimum and maximum temperatures (°C) during the 2015–2016 and 2016–2017 growing seasons (October–August) in the IT-LAZ test site.

2.1.2. IT-VE

The study site IT-VE is situated in Northern Italy (Figure 1), specifically in the Veneto region near the Ceregnano municipality (study site central coordinates 45°.30′ N and 11°51′ E, 5 m above sea level, Datum WGS84). It is a part of the experimental farm "Sassi Rami" belonging to Veneto Agricoltura, an agency dedicated to innovation in the primary sector by conducting supportive activities for the Regional Council in the agricultural, agri-food, forestry and fishing sectors. Typical cropping systems in this area consist of winter cereal and irrigated summer crops, predominantly maize, soybean, forage crops, vegetables and fruit trees. The site experiences an average temperature of 14 °C and an annual rainfall of 500 mm, with a dry period prevalent during the summer months.

- in situ MS data at 10 cm

in situ soil moisture measurements were continuously acquired at a 1-h sampling frequency, using a cosmic ray neutron sensing (CRNS) probe, also known as Finapp3. Specifically designed for agro-hydrological applications, the measurements were conducted from 5 March 2021 to 10 December 2021 over an irrigated soybean field with a surface area of around 14 ha (field number 3 in Figure 1). The Finapp3 possesses a large horizontal

footprint (i.e., the area detected by the sensor) of tens of hectares and has a depth of penetration ranging from 10 cm to up to 50 cm into the soil. More details about the CRNS Finapp3, the experimental setup and the preprocessing procedure to derive soil moisture from Raw Neutron Counts can be found in Stevanato et al. [21] and Gianessi et al. [22]. Stevanato et al. [21] also provide supplementary material (data collected and processed at six experimental sites), which includes data for our study site. According to the World Reference Base for soil resources (WRB 2014), the primary soil type of the soybean field is classified as fluvic Cambisol, which originates from the Holocene River deposit, where a sandy fluvial deposit traverses the loamy field.

- Temperature and precipitation data

To describe the weather trend, daily meteorological data were obtained from the regional environmental agencies (ARPAV) data repository. A climate station is located in Sant Apollinare (Rovigo), approximately 3 km westward from the study area's central point. The climatic trend remained generally consistent with historical records in terms of both rainfall and temperature (Figure 4).

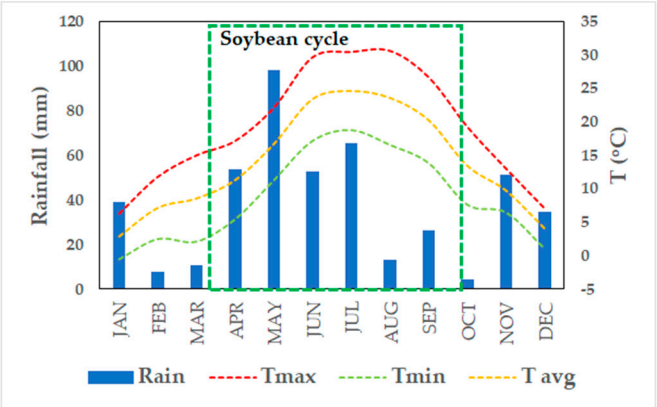

Figure 4. Monthly rainfall (mm) with average, minimum and maximum temperatures (°C) during 2021 for IT-VE study site.

2.2. S²MP Soil Moisture

Several approaches were proposed to estimate soil moisture in agricultural environments from Sentinel-1 data [2,4]. While the C-band radar has proven effective in estimating soil moisture, the reliance on Sentinel-1 data from Copernicus arises primarily due to their status as the only freely accessible SAR data available at present.

In our analysis, we employed the S²MP (Sentinel-1/Sentinel-2-derived soil moisture product at plot scale), a soil moisture product developed by El Hajj et al. [4] by coupling Sentinel-1 SAR data and Sentinel-2 optical data. In the best of our knowledge, the S²MP is the only operational plot-scale soil moisture product derived from S1 data currently available for users. In addition to the fine spatial resolution of the S²MP, previous comparative studies among various S1-derived SMs consistently highlighted the superior performance of S²MP, providing the most robust SM estimations compared to its competitors [13,23]. To estimate the SM values within the S²MP, El Hajj et al. [4] inverted the Water Cloud Model (WCM) using C-band parameterized by Baghdadi et al. [24] mainly for winter crops and grasslands. To estimate SM, El Hajj et al. [4] used a fully connected neural network (NN) comprising two hidden layers, each with 20 neurons. Linear and tangent-sigmoid transfer functions were associated with the first and second hidden layers, respectively. The inversion approach to estimate SM uses the VV polarization or both VV and VH polarizations. However, the enhancement in SM estimation accuracy by incorporating both VV and VH polarizations was limited compared to the use of only VV [4]. Comprehensive description of the used NN is provided by El Hajj et al. [4]. Alongside the radar backscattered signal, the NN uses the SAR incidence angle, and the NDVI derived from Sentinel-2 images as in-

puts. The S^{2}MP maps are specifically generated for agricultural areas, excluding vineyards and orchards.

In this study, the NN algorithm used in the S^{2}MP product was employed to estimate the SM for our experimental plots. Both ascending (A) (around 6 p.m. UT) and descending (D) (around 6 a.m. UT) S1 acquisitions were utilized in this study for estimating soil moisture. The S1 data, freely available from the European Space Agency's (ESA) website (https://dataspace.copernicus.eu/ (accessed on 20 December 2023)), had a revisit time of 12 days for 2016 and 6 days after 2017. For both sites, the studied fields were covered by three different S1 orbits. Figure 5 illustrates the temporal distribution and the overall coverage of the S1 orbits for each site-year. The incidence angle for fields on the IT-LAZ site was 35°, 38° and 45° for orbits D95, A15 and A117 for both 2016 and 2017, respectively. For fields at the VE site, the incidence angle was 31°, 39° and 41° for orbits D168, D95 and A117, respectively.

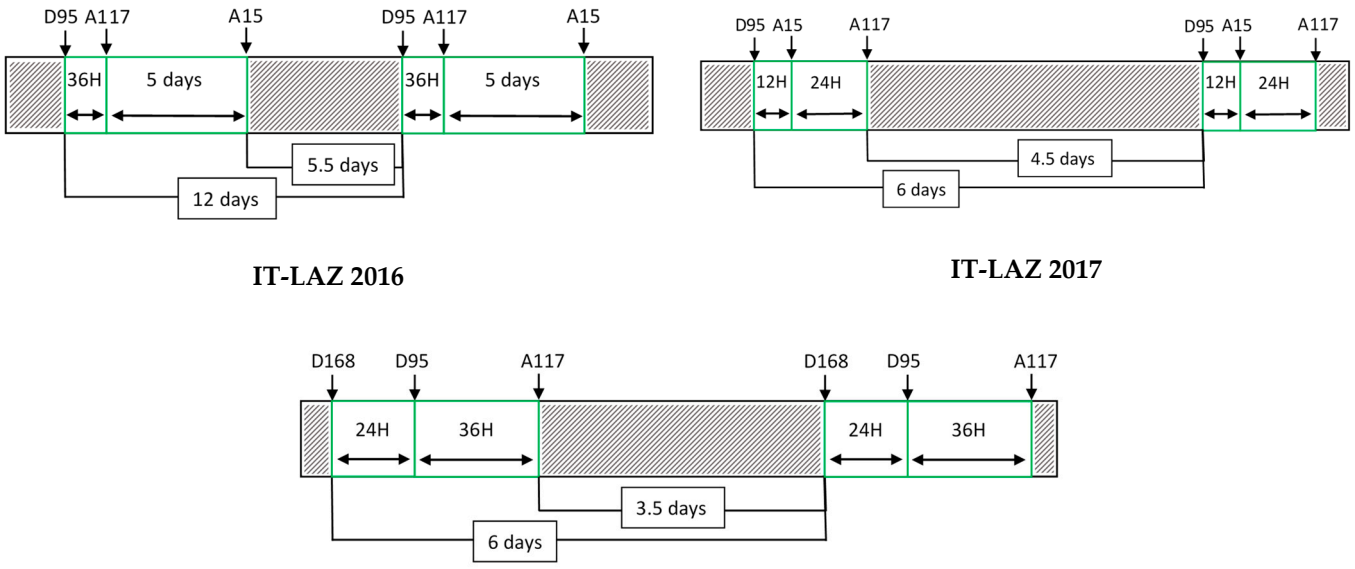

Figure 5. Frequency of S1 images in "ascending" (A) and "descending" (D) acquisitions for all orbits covering our reference fields in IT-LAZ and IT-VE. The hatched area represents the period with no S1 acquisitions. Numbers next to "D" and "A" represent the S1 orbit acquisition number.

The S1 images were calibrated using the S1 toolbox developed by ESA. Calibration involves a two-step process: the first step is radiometric calibration, which converts a digital number into a backscatter coefficient, σ°, in linear units; the second step is geometric correction, which involves ortho-rectification, using a digital elevation model at 30 m from the Shuttle Radar Topography Mission (SRTM). As the comparison was conducted at the plot scale, the average S1 signal of all the pixels within each plot and at each available S1 image was computed to derive a singular representative value for each plot. An interior buffer of −10 m (one pixel) was applied for the plots' boundaries to exclude border pixels of the plot from the mean calculation.

In addition to Sentinel-1 images, all cloud-free Sentinel-2 (S2) optical images over each study site/year were obtained from the Theia website (https://www.theia-land.fr/ (accessed on 20 December 2023)). The S2 images provided by Theia are corrected for atmospheric interference and so are called Level-2A products. S2 images were mainly used to calculate the NDVI needed for the SM inversion by the NN.

2.3. Methods

Using the NN of the S^{2}MP and employing all available S1 images, a time series of SM estimates was generated for each crop cycle within each plot. All collected S1 images from several orbits were combined into one time series dataset regardless of the specific orbit number and its associated incidence angle. For the comparison between the in situ measured SM and estimated SM, only common dates between the measured and estimated SM were used for each plot by considering the SM measurement of the common date, at the same hour of the S1 acquisition hour.

In the literature, several studies have outlined many limitations in the S1 C-band SM estimations, including but not limited to, the failure of estimating soil moisture when the vegetation of certain crops is highly developed [18,25,26], the sensitivity of the C-band radar signal only to the first cm of the soil [27] and the need to have low incidence angles for optimizing the estimation of soil moisture [28], as well as the difficulty of correctly estimating moisture content for soils with very high or very low roughness [9,29].

In this paper, our analysis concentrates on three key aspects:(1) investigating the mismatch between the in situ SM measurements at 10 cm and the S1-derived SM estimates, using the C-band; (2) assessing the effect of the vegetation cover of certain crops on the quality of soil moisture estimates; and (3) examining the influence of the S1 acquisition configuration, specifically the S1 incidence angle, on the SM estimates. To comprehensively assess these aspects, we examine first the temporal evolution of the estimated and 10 cm measured soil moisture for each crop type. Then, we evaluate the difference between the estimated and measured SM, using the conventional statistical metrics, including the RMSE, bias and correlation coefficient (R), while concentrating on differences due to the vegetation development of each crop (by means of NDVI) and the soil humidity conditions. Subsequently, we analyze the influence of the S1's incidence angle on the SM estimates. Finally, the study offers a synthetized summary of the strengths and limitations of the estimated S1 soil moisture for the different studied crop types.

3. Results

3.1. Temporal Series Analysis

This section presents a time series analysis of the S^{2}MP-estimated SM with the in situ SM (at 10 cm depth) for tomato, wheat, cover crops and soybean.

3.1.1. Tomato Crop Case

For the tomato crop cycle in 2016, discords between estimated SM and in situ SM were observed in the beginning of the crop cycle, specifically between 10 May and 23 May 2016. During this period, the vegetation was not well developed, with NDVI values ranging between 0.2 and 0.3, while the estimated SM was notably lower than the in situ SM by 18 to 22 vol.%. The C-band S1 signal estimated the SM to be between 7 and 14 vol.% during this period, compared to in situ soil moisture between 29 and 32 vol.% (at 10 cm in depth). No rainfall was recorded during this period, and the surface SM was probably lower than the 10 cm depth SM, which led to an underestimation of the S1 SM on 10, 11 and 16 May by approximately 21 vol.%. A rain accumulation of 15 mm between 17 and 19 May was noted, followed by a dry period between 20 and 23 May. S1 underestimated the SM on 22 and 23 May by about 18 vol.%. From 23 May to 28 May, the in situ SM showed a considerable decrease (from 32 vol.% to 24 vol.%), whereas the S1 SM on 28 May (20 vol.%) was close to the in situ SM at a 10 cm depth (24 vol.%), probably due to the similar SM levels at the surface and 10 cm depth.

Irrigation for this field started at the end of May with the first irrigation event occurring on 29 May, resulting in an increase in the in situ SM at 10 cm of depth from 24 vol.% to 32 vol.%. However, between 29 May and 4 June, in situ SM decreased from 32 vol.% to 24 vol.% and S1 SM were lower than in situ SM by 6 vol.%. The second irrigation event, recorded on 9 June, led to similar SM in surface and at 10 cm depth where the S1 SM on 9 June reached 28.1 vol.% closely similar to in situ SM (27.6 vol.%).

Between 13 June and 29 July, regular irrigation events occurred at an average interval of every 3 days. With regular irrigation events, the bias between the 10 cm in situ SM and the S1 SM decreased. However, it was noticed that when the time gap between S1 acquisition dates and the irrigation events dates is of 2 or 3 days, the difference between S1 SM and in situ SM ranged between 4 and 7 vol.% against 1 to 2 vol.% for dates where the delay between irrigation and S1 acquisition was 1 day or less.

Between 15 June and 27 July, corresponding to a high NDVI (between 0.62 and 0.76), S1 overestimated the in situ SM. This could probably be attributed to the presence of fruits accompanied by an increase in the vegetation water content, resulting in an increase in the backscatter S1 signal. Indeed, the emergence of fruits is not accounted for in the WCM, used in the inversion process of the S1 estimates, thus making it difficult to compensate the effect of the fruits in the SAR backscattering coefficients.

For the tomato crop cycle in 2017, available data were restricted to the period of developed tomato cover in June and July 2017 (NDVI between 0.5 and 0.6) (Figure 6b). During this period, no significant rainfall events were recorded, except for a slight rain accumulation of 4 mm and 1.5 mm on 28 June and 30 June 2017, respectively. However, regular irrigations were carried out during the tomato growing season between June and July, leading to the in situ SM varying between 28 and 34 vol.% at a 10 cm depth. The comparison between S1 SM and in situ SM showed estimated moistures lower than the in situ moistures by about 3.7 vol.%. Only for 10 June, a slightly higher difference between S1 SM and in situ SM was observed (underestimation by S1 of 8 vol.%), most probably due to the delay between the irrigation event (8 June) and S1 acquisition date (10 June). In this field, continuous irrigation kept the soil consistently wet at both the surface and a 10 cm depth, resulting in minimal differences between S1 SM and the 10 cm depth in situ measurements.

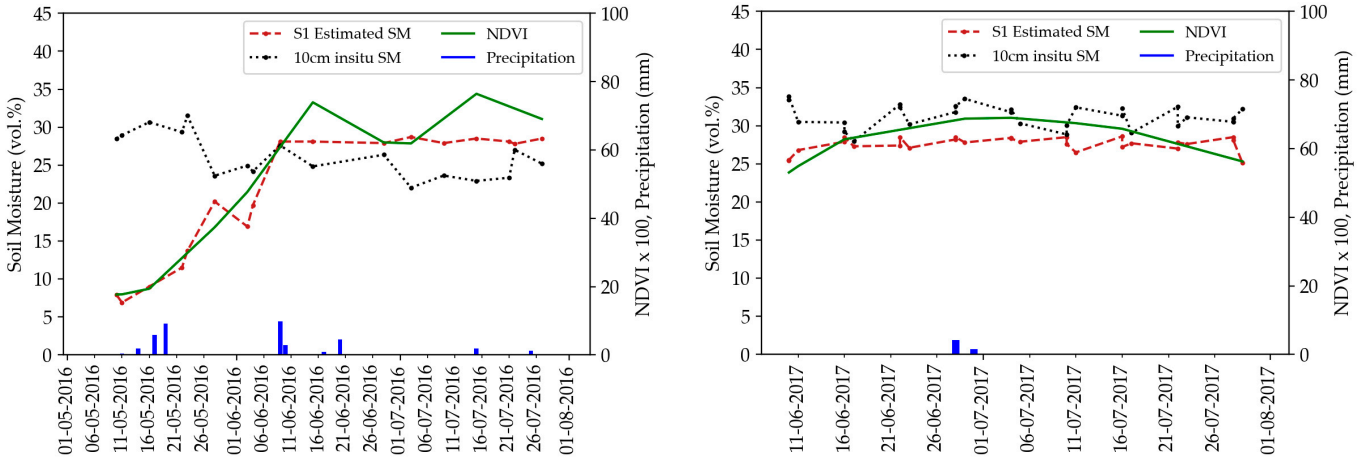

(**a**) (**b**)

Figure 6. Temporal variation in the in situ 10 cm measured SM (black dotted line) and the S1 estimated SM (red dashed line) for (**a**) tomato crop cycle in IT-LAZ 2016 and (**b**) tomato crop cycle in IT-LAZ 2017. The NDVI is represented by a solid green line on the right *y*-axis, along with precipitation (blue line).

3.1.2. Wheat Crop Case

For the first wheat cycle (Figure 7a), no precipitation occurred between 5 and 15 February 2016. The surface soil moisture estimated by the C-band radar signal appeared drier than the 10 cm in situ soil moisture, with a difference reaching an order ranging between 10 and 16 vol.%. This indicates that the soil moisture estimated from the S1 C-band is strongly underestimated during the dry period compared to in situ SM at 10 cm due to the possible rapid dry-out of the surface SM compared to the deeper soil moisture. The rainfall accumulation of 14 mm on 16 and 17 February led to an underestimation of the SM by 6 vol.% when only using the S1 images acquired on these dates.

On 27 and 28 February 2016, nearly 25.8 mm of accumulated rainfall was recorded. The surface soil should be wet during these two days, which was illustrated by the estimated SM on 28 and 29 February (25 vol.%). However, the estimated SM levels for these two days remain lower than the in situ SM at a 10 cm depth, which reached about 35 vol.%. A similar trend was observed for the S1 image from 05 March 2016, with an underestimation of the SM by S1, despite a rainfall of 13.4 mm on the same day (22 vol.% by S1 against 34 vol.% measured). This difference could be due to the attenuation of the radar signal by the vegetation at this time of year (NDVI > 0.8 for both February and March images), causing very low soil contribution in the S1 backscattering signal. In addition, the underestimation observed between the in situ and estimated SM in these very wet conditions could be due to a limitation of the SM inversion approach in the case of high soil moisture values, as the radar signal starts to decrease with very high soil moisture values at a threshold of 30–35 vol.% (extremely wet soil conditions). The light rainfall of 8 and 9 March 2016 (accumulation of 10.2 mm) did not allow for a good estimation of the SM on the S1 image of 11 March 2016, where the S1 SM was underestimated by 18 vol.%, corresponding to a NDVI value reaching 0.9.

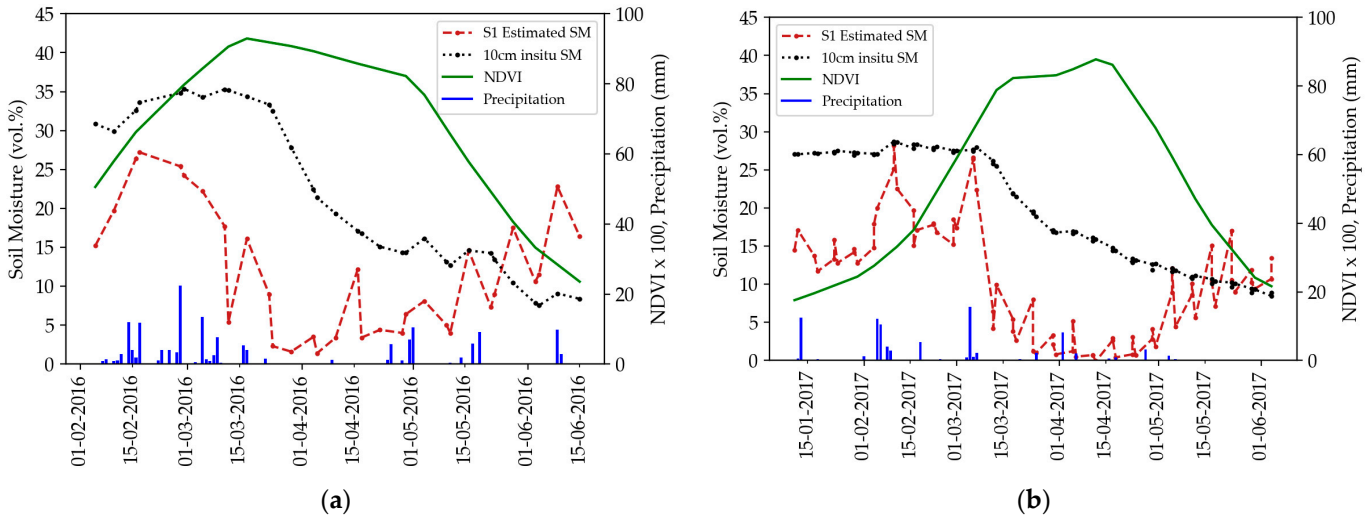

Figure 7. Temporal variation in the in situ 10 cm measured SM (black dotted line) and the S1-estimated SM (red dashed line) for (**a**) wheat crop in IT-LAZ 2016 and (**b**) wheat crop in IT-LAZ 2017. The NDVI is represented by a solid green line on the right *y*-axis, along with precipitation (blue line).

On 12 March, the underestimation of the S1 SM reached its maximum order (underestimation of about 30 vol.%) due to the total attenuation of the S1 signal by the vegetation cover (NDVI about 0.9), leading to the full absence of soil contribution in the S1 backscattered signal in the C band. The accumulated rainfall of about 9.4 mm on 16 and 17 March 2016 led to an increase in the estimated SM from 5.4 vol.% on 12 March to 16.1 vol.% on 17 March but remained underestimated by 18 vol.% compared to the in situ 10 cm SM. Until the beginning of May, the estimated moisture remained less than 5 vol.% compared to the in situ SM, reaching 30 vol.%, reflecting a complete vegetation attenuation to the S1 signal during the heading phase of the wheat crops.

From 16 May, vegetation water content decreases were accompanied by a low NDVI (0.58 on 16 May and 0.23 15 June), and the in situ SM at 10 cm showed a decrease from 14 to 8 vol.%. For this last period, the difference between the estimated and in situ SM decreased to an order of 6.8 vol.%.

The same trend of soil moisture estimation could be observed on the second wheat plot in 2017 (Figure 7b). From 11 January 2017 to 4 February 2017, the SM levels estimated by S1 are lower than those estimated by in situ SM by about 12 vol.% due to lower SM values at the surface than that at a 10 cm depth in the absence of rainfall. Due to the precipitation on 5, 6, 8 and 9 February (about 30 mm), surface SM and in situ SM at 10 cm depth were

most likely close during the S1 acquisition dates. As a result, the S1 SM estimations became close to the in situ SM at 10 cm depth with a difference of about 4 vol.% on 5, 10 and 11 February 2017.

Similarly, the rainfall accumulation of 16 mm on 5 March 2017, reduced the difference between surface SM and SM at 10 cm depth leading to very good estimation of the soil moisture on 6 March with a difference of 1 vol.%. On 7 March, S1 SM showed less agreement with the in situ SM than that on 6 March, with a difference of about 5.5 vol.% due to the dry-out of the surface soil 2 days after the date of the last rainfall event.

From 12 March, the soil contribution in the S1 signal became negligible (NDVI higher than 0.8) due to the high attenuation by the vegetation, leading to a high underestimation of the SM by 8 to 22 vol.% compared to the measured SM. After the 5th of May, the NDVI started to decrease, with NDVI values reaching 0.6 on 5 May and 0.2 on 4 June. The attenuation of the S1 signal by the vegetation decreased, and, therefore, the estimation of the SM by S1 became more accurate, with an accuracy higher than 4 vol.%.

3.1.3. Cover Crop Case

For the first studied cover crop cycle (Figure 8a), the NDVI values between December 2015 and April 2016 varied between 0.62 and 0.88. In addition, the accumulated precipitation during this same period was relatively low, with some rainfall events of 12 mm (except on 28 February, with 22 mm). The estimated soil moisture was, on average, 8 vol.% lower than the in situ soil moisture at a 10 cm depth. The lower S1 SM values could be due to high vegetation development (high NDVI values), leading to the high attenuation of the radar signal in the C band and lower soil contribution.

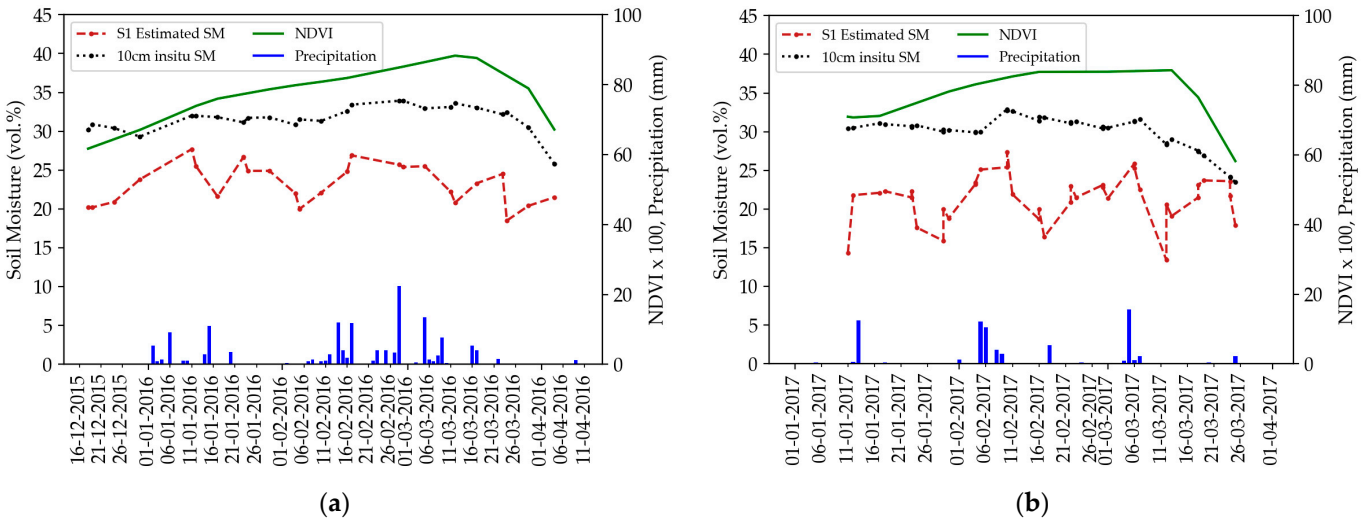

Figure 8. Temporal variation in the in situ 10 cm measured SM (black dotted line) and the S1 estimated SM (red dashed line) for (**a**) cover crop in IT-LAZ 2016 and (**b**) cover crop in IT-LAZ 2017. The NDVI is presented in solid green line on the right y-axis along with precipitation (blue line).

The most accurate estimation of the SM from S1 was obtained on the last day of our time series, on 4 April 2016 (difference between S1 and in situ SM equal to 4 vol.%), which corresponded to the lowest in situ SM at 10 cm in depth (26 vol.%) and moderate NDVI (0.67). In this case, we assume that this was probably due to the possible low difference between the in situ SM at 10 cm in depth and the SM at the surface (part corresponding to S1 estimation), as well as to the lower NDVI value (lower attenuation of the soil contribution by the vegetation cover).

The same trend is present for the second cover crop field (Figure 8b), with a SM underestimation of about 9 vol.% (in average) during the period between 11 January 2017 and 13 March 2017, accompanied by NDVI values increasing from 0.61 to 0.84 during this

period. Similar to the cover crop in 2016, the most accurate estimation of SM from S1 was obtained for the moderate NDVI values (between 0.58 and 0.61) after 15 March 2017, where the difference between S1 and in situ SM was lower than 5 vol.%.

3.1.4. Soybean Crop Case

For the soybean plot (Figure 9), no rainfall events were noted between 9 March and 9 April 2021, and the soil moisture at a 10 cm depth decreased from 20 vol.% to 13 vol.%. For this period, NDVI values varied between 0.55 and 0.73, with a slight underestimation of about 2 vol.% for the S1 estimates. On 12 April, a rainfall event of 16 mm was recorded which led to an increase in the SM at 10 cm of depth. From the S1 images acquired on 13–15 April, we can see that the estimated SM values were close to the SM measurements, with a difference of less than 5 vol.%.

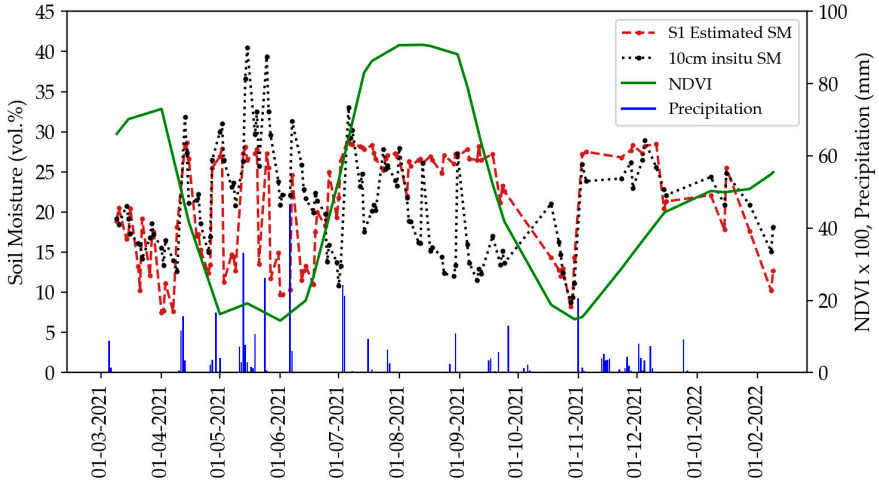

Figure 9. Temporal variation in the in situ 10 cm measured SM (black dotted line) and the S1 estimated SM (red dashed line) for soybean in IT-VE 2021. The NDVI is presented in solid green line on the right *y*-axis, along with precipitation (blue line).

Between 19 and 26 April 2021, the study site did not experience any rainfall event, and the estimated soil moisture decreased to values between 12 and 17 vol.% lower than the in situ SM at a 10 cm depth by 4 vol.%. Between 26 and 29 April, a precipitation accumulation of 22 mm was recorded, rendering the soil well wet, with the SM at the 10 cm depth being 30 vol.%. The S1 SM for the three S1 images acquired between 27 April and 2 May was about 27 vol.%, showing a good estimation of the soil moisture by S1 and probably a similar SM in the topsoil surface and at a 10 cm depth, with low attenuation of the soil contribution due to the low vegetation cover having an NDVI value of about 0.17.

The heavy rainfall that started on 13 May (33 mm), the same day as S1 acquisition, led to high estimated soil moisture on 13 May (26 vol.%) and reduced the difference between the SM at the surface and the SM at 10 cm in depth. The estimation of the SM from the S1 image on 13 May (27 vol.%) was close to the in situ SM (26 vol.%). On 14 and 15 May, the SM recorded at 10 cm in depth was about 40 vol.%. However, for 14 and 15 May, the SM values estimated by S1 were lower than the in situ SM by 11 vol.%. This could also be attributed to the low sensitivity of the SAR signal for very wet soil moisture conditions beyond 30–35 vol.%.

The rainfall on 19 May (11 mm) resulted in similar SM at the surface and at a 10 cm depth, leading to a good estimation of SM from S1 images on 19 and 20 May (slight underestimation on 20 May by 4.5 vol.%). On 21 May, two days after the rainfall event of 19 May, the soil dried at the surface, and the S1-estimated SM was 12 vol.% lower than the SM at a 10 cm depth. The precipitation on 24 May (26 mm) made the soil very wet at the surface, as well as at the 10 cm depth, with an SM value of 39 vol.%. However, due to the

saturation of the radar signal for SM values higher than 30 vol.%, the S1 SM on 25 May was underestimated by 12 vol.%.

Between July and October, the time series of the estimated SM showed an approximately constant high-order estimation of the SM, reaching 27 vol.%, despite the important variation observed in the in situ SM at 10 cm, ranging between 30 vol.% to 10 vol.%, according to dry and wet conditions due to rainfall or irrigation. These constant estimations of high order mainly corresponded to NDVI values above 0.6 for the soybean. These high overestimations are most likely due to the high vegetation contribution in the S1 signal that increases the backscattering signal and dominates the soil contribution, causing the SM estimates to be unreliable.

3.2. Differences between Measured and Estimated SM

The RMSE, bias and correlation coefficient (R) between the 10 cm in situ soil moisture and the S^2MP estimated soil moisture were calculated for each crop type for two NDVI classes separately: (1) NDVI less than 0.7, representing low-to-moderate vegetation cover; and (2) NDVI greater than or equal 0.7, signifying dense vegetation cover (Table 2). The three metrics were also computed for all crop types grouped together (labelled "All Data" in Table 2) for the two NDVI classes to present the overall accuracy.

Table 2. RMSE, bias and correlation coefficient (R) calculated for each crop type for low-to-moderate vegetation (NDVI < 0.7) and dense vegetation (NDVI > 0.7). All data rows show the three metrics calculated by grouping all data together for each NDVI class separately.

Crop Type	Low-to-Moderate Vegetation Cover (NDVI < 0.7)			Developed Vegetation Cover (NDVI ≥ 0.7)		
	RMSE (vol.%)	**Bias (vol.%)**	**R**	**RMSE (vol.%)**	**Bias (vol.%)**	**R**
Wheat	8.6	−5.4	0.65	16.6	−15.5	0.67
Cover crop	7.0	−6.1	0.01	9.4	−8.9	0.37
Tomato	11.72	−10.6	0.23	3.7	−1.0	−0.34
Soybean crop	7.4	−1.84	0.46	7.5	4.1	0.32
All data	7.9	−3.9	0.59	11.5	−6.0	0.48

For an NDVI less than 0.7, the general RMSE reached 7.9 vol.%, with a moderate underestimation (bias) of −3.9 vol.% and good correlation coefficient reaching 0.59. However, the bias value showed considerable variability across the crop types. While moderate underestimation is observed for wheat, cover crops and soybean (between −6.1 and −1.84 vol.%), notably high underestimation is observed for the tomato crop (−10.6 vol.%). This high underestimation observed for the tomato crop, even with low vegetation cover, is mainly due to the dry soil conditions observed at the beginning of the crop cycle (Figure 6a,b), where the S1-estimated SM values were largely lower than the 10 cm in situ SM. For dense vegetation cover (NDVI > 0.7), a generally higher underestimation is observed (grouping all data), with a bias of −6.0 vol.%. However, drawing conclusions on only this overall bias is misleading due to the notable variability of the bias values having opposite signs between the crop types. Where wheat and cover crops showed extremely high underestimation (bias = −15.5 vol.% and −8.9 vol.%, respectively), the soybean crop showed positive bias values (4.1 vol.%), indicating an overestimation of the SM by S1 compared to the in situ soil moisture. Contrary to wheat crops where the SM is underestimated for developed vegetation cover due to the S1 attenuation by wheat kernels and absence of soil contribution in the S1 backscattered signal, the soybean showed an overestimation due to the high contribution of the soybean fruits in the backscattered S1 signal. For the tomato crop, the underestimation observed for low-to-moderate vegetation (NDVI < 0.7) decreased to reach −1.0 vol.% for dense vegetation cover (NDVI > 0.7). This better bias value for dense cover compared to low vegetation could be due to the combined effect of

both wetter conditions caused by frequent irrigation episodes and to the contribution of the tomato fruits in the backscattered S1 signal that increased the S1 backscattering values.

Since the difference between the measured and estimated soil moisture may vary due to the combined effect of both the soil moisture conditions (dry to slightly wet and very wet) and the vegetation development, we recalculated the bias values by considering two classes for soil moisture conditions (dry to slightly wet and very wet) and several classes for NDVI. The boxplots in Figure 10 present the distribution of the differences between the S1-estimated SM and the 10 cm measured SM (bias = estimated − measured) for different NDVI intervals grouped according to two soil moisture conditions: dry to slightly wet soil moisture at 10 cm (SM $\leq$ 20 vol.%) and humid conditions with SM > 20 vol.%.

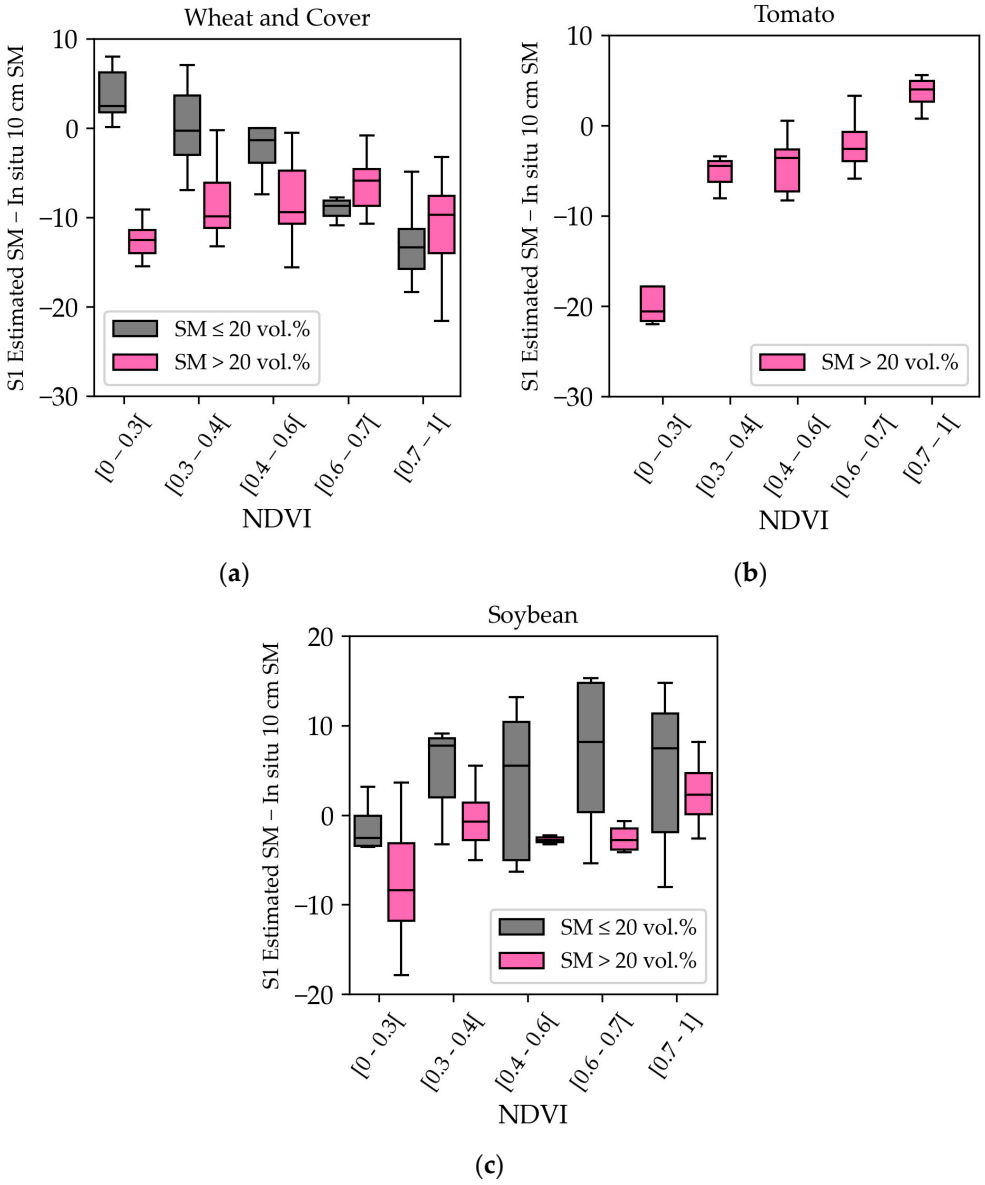

Figure 10. Boxplots of the distribution of the difference between the S1 estimated SM and the 10 cm in situ SM for different NDVI intervals and two soil moisture classes (SM > 20 vol.% in rose) and (SM $\leq$ 20 vol.%) in grey for (**a**) wheat and cover crops, (**b**) tomato and (**c**) soybean.

In Figure 10a (case of wheat and cover crops), we noticed that the bias value for bare soil conditions (0 < NDVI < 0.3) is positive, ranging between 0 and 8 vol.%, with a median value of 2.5 vol.% (slight overestimation of the SM by S1). The underestimation then increases as the NDVI increases, reaching a median value of −1.5, −8.7 and −13.6

(negative bias signifies underestimation) for NDVI classes between 0.4 and 0.6, between 0.6 and 0.7 and finally greater than 0.7, respectively. As shown in Figure 7a,b, for the wheat crops, the SM estimates from S1 vanished with high NDVI values due to the very low soil contribution in the S1 C-band backscattering signal caused by the high attenuation of the developed wheat vegetation cover. For wet conditions (pink boxplots with SM > 20 vol.%), the bare soil class (NDVI < 0.3) showed a high underestimation of the SM (median value of −12.5 vol.%), which could be due to the decrease in the S1 signal for extremely wet soil conditions (beyond 30 vol.%). For other NDVI classes, similar behavior is noticed with a median underestimation of about −9 vol.% for other NDVI classes in the case of wet soil conditions.

For the tomato crop, the measured soil moisture at 10 cm did not decrease beyond 20 vol.%. The boxplots in Figure 10b show a median bias value of −20.6 vol.% for very wet bare soil (SM > 20 vol.%), similar to that noticed for wheat plots. The presence of topsoil slaking crust or a mulch could also be a reason for the reduction in the drying rate of the 10 cm depth, leading to a high difference between the 10 cm depth SM and the topsoil-measured SM values. With the development of the canopy cover, the bias decreased and attained a median value of −4.4, −3.5 and −2.6 vol.% for NDVI classes between 0.3 and 0.4, between 0.4 and 0.6 and between 0.6 and 0.7, respectively. This decrease in the bias could be related to the frequent irrigation application on the tomato plots that maintained a consistent soil moisture value at the surface and at 10 cm in depth, leading to less of a difference between the estimated SM at the surface and the measured SM at a 10 cm depth. For NDVI values greater than 0.7, S1 overestimated the 10 cm depth soil moisture (median bias value of 4.1 vol.%), which could probably be due to the increase in the S1 backscattering signal with the presence of tomato fruits for developed tomato crop cover, as shown mainly in Figure 6a. The emergence of fruits for some crop types, such as the tomato, increases the C-band backscattering signal due to the geometrical structure of the plant (fruits and leaves), causing an increase in the SM values. It is good to mention that the WCM used for the SM estimates did not include a description of the crop type or plant structure; thus, the effect of the crop fruits to the S1 backscattering signal (increasing signal in the case of tomato) was not evaluated.

For the soybean crop (Figure 10c), a similar underestimation of very wet soil is observed for all the NDVI classes as that of the wheat and tomato. For dry soil with medium-to-high NDVI values (NDVI between 0.6 and 0.7 and NDVI greater than 0.7), we noticed that the S1 SM estimates overestimate the 10 cm SM measurements with a bias median value reaching 8.1 and 7.5 vol.%. As shown in Figure 9, the estimated SM values for the soybean plot between July and October 2021 were approximately constant at high values (between 25 vol.% and 27 vol.%) despite the variation in the measured SM at 10 cm that decreased gradually during the absence of rainfall and increased after a rainfall event. The overestimation (with constant saturated values) for the soybean plot with developed vegetation cover is mainly linked to the soybean geometrical structure of the plant when it is well developed, which increases the C-band backscattering signal and yields an overestimation of the SM values.

3.3. Effect of the Radar Incidence Angle

In this study, we tried to investigate the effect of the incidence angle by taking advantage of having three main groups of incidence angles: less than 35° (SM estimates with low incidence angle, ~31°), between 35° and 40 ° (SM estimates with moderate incidence angle of ~35°, 38° and 39°) and greater than 40° (SM estimates with high incidence angle, ~41° and 45°). For each incidence angle class, the average difference between the S1-estimated and 10 cm measured SM was calculated using all the available SM estimates with an NDVI less than 0.7. We excluded SM measurements with an NDVI greater than 0.7 to avoid mixing the SM error estimates due to the developed vegetation cover in order to concentrate on the effect of incidence angle only. Figure 11 shows the average difference between estimated and 10 cm in situ SM (estimated—in situ) for the three incidence angle classes.

The figure demonstrates that the average difference between the estimated and measured SM decreases from −3.5 vol.% for a low incidence angle (less than 35°) to −7.1 vol.% for a moderate incidence angle between 35° and 39° to reach the biggest difference of −8.5 vol.% for an incidence angle greater than 40°. These results prove that a better estimation of the SM from the C-band S1 could be obtained at mainly low-to-moderate incidence angles, whereas high incidence angles can yield higher anomalies.

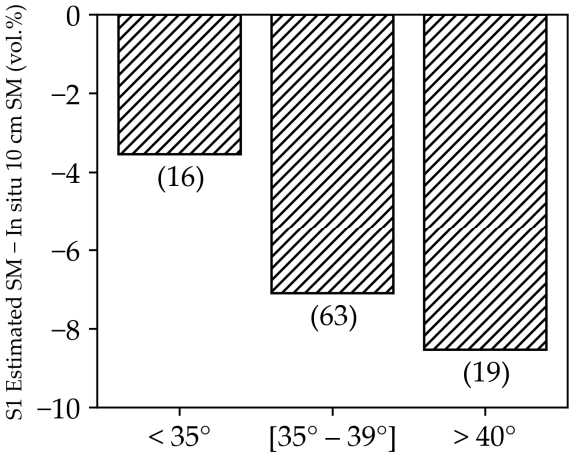

Figure 11. Average difference between S1-estimated SM and 10 cm in situ SM for three incidence angle classes: less than 35°, between 35° and 39° and greater than 40°. Numbers below each bar correspond to the number of the SM estimations used to calculate the average difference. Only SM estimates with a corresponding NDVI value less than 0.7 were considered.

4. Discussion

4.1. Soil Moisture at Different Depth Layers

The analysis of the S1 SM estimates for the soil layer between 0 and 5 cm, using the C-band, demonstrated a general underestimation of the SM values at 10 cm, except for special cases with wet conditions when the topsoil layer and the 10 cm layer may have similar soil moisture levels. To understand the difference between the topsoil-estimated SM and the 10 cm measured SM, an assessment was conducted by comparing the in situ measurements taken at 10 cm with in situ obtained from a deeper soil layer at 20 cm. The objective here is to analyze whether the underestimation of the S1 SM compared to the 10 cm measured SM is only due to the difference in the soil water content between soil layers or is related to an artifact in the S1-estimated SM. The histogram in Figure 12 shows the distribution of the difference calculated between 10 cm and 20 SM measurements (in situ) for all the plots (bias = 10 cm in situ SM–20 cm in situ SM).

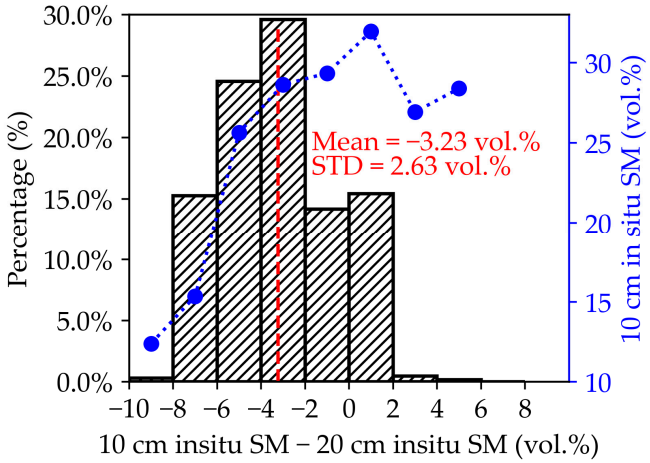

Figure 12. Histogram of the distribution of the difference between the measured in situ soil moisture at 10 cm and 20 cm (SM at 10 cm–SM at 20 cm SM) for all studied plots. In blue, toward the right *y*-axis, is the average value of the measured 10 cm soil moisture corresponding to each bar of the histogram.

The histogram clearly shows that the 10 cm measured SM is lower than that at 20 cm, with an average difference of −3.2 vol.% and a standard deviation of 2.6 vol.%. Furthermore, 69.4% of the measured SM at 10 cm had a difference ranging between −10 vol.% and −2 vol.% compared to the SM at 20 cm, while 83.6% of the measured SM at 10 cm was less than that at 20 cm (difference < 0). The blue line, representing the average 10 cm SM values for each bin (average SM for all measurements corresponding to in each bar), highlights that a high negative difference between 10 cm and 20 cm occurs for the dry soil, where the difference of less than −6 vol.% occurs for SM values of less than 12 vol.%. As the 10 cm soil layer becomes wetter (potentially due to rainfall or irrigation), the difference between the 10 and 20 cm SM values decreases to reach a difference between −2 vol.% and 0 vol.% for an SM average value around 30 vol.% (extremely wet conditions). Only a few measurements were found with a slightly positive bias (between 0 and 2 vol.%), also corresponding to extremely wet conditions (SM greater than 30 vol.%). Similar results were shown by Dong et al. [30], who similarly compared soil moisture measurements between 5 cm and 10 cm depths. They reported that soil moisture at the 10 cm depth could be 5.9 vol.% higher than that at the 5 cm depth.

The histogram of the difference between the 10 and 20 cm layer strongly suggests that the underestimation between the topsoil (0–5 cm) S1 SM estimates and the 10 cm measured SM could be majorly due to the different soil water content related to the soil depth. For dry conditions, the topsoil layer dries rapidly due to evaporation and faster than the 10 cm depth SM, and this could be the reason for the underestimation observed in this study. An additional reason could be that the 10 cm depth dries slower than the topsoil due to the possible surficial soil crust, leading to a slower drying rate for the 10 cm SM compared to the topsoil SM. This mainly can happen for silty topsoil with low soil organic carbon content. In this context, the soil texture with variable percentages of clay, silt and sand also plays an important role in the variability of SM values between the different soil layers [31]. Moreover, the field work, such as the application of chemical fertilizer combined with harrowing, can impact the difference between the topsoil SM and the 10 cm depth, leading to a higher drying rate for the topsoil. As the soil becomes wet, the underestimation decreases since, with humid conditions, the topsoil and 10 cm depth soil moisture could be at the same order of magnitude. However, the effect of extremely wet conditions that decrease the S1 signal could also lead to an underestimation of the SM values using the S1 in that case.

4.2. Limitations of S1 SM Estimations

As previously mentioned, most studies have conducted a broad assessment of S1 SM retrieval without specifically considering additional constraints within the evaluation process. Consequently, only a limited number of studies have addressed the impact of vegetation development and soil moisture conditions on S1 SM estimations. Unlike our study, there have been few comprehensive evaluations regarding the influence of vegetation development across various crop types on S1 SM retrieval previously presented. In a study conducted by Dabrowska et al. [32], the WCM was calibrated to estimate soil moisture at the plot scale in Central European grassland and marshland sites (wetlands), utilizing NDVI as a vegetation descriptor. In their study, they compared the S1 backscattered signal in VV and VH polarizations with in situ soil moisture depths of 5, 10 and 20 cm and showed that the correlation coefficient between S1 backscattering and in situ SM decreases with the increasing soil depth. The highest correlation was obtained between S1-VV and in situ SM measured at the 5 cm soil depth, particularly with ascending S1 orbits exhibiting low incidence angles (~35°). Regarding NDVI, their results illustrated a reduction in the sensitivity of S1-VV to 5 cm in situ SM for NDVI values exceeding 0.78, reaching a minimal correlation between VV and 5 cm in situ SM, with diminishing sensitivity (R = 0.19 and 0 dB/vol.%). Balenzano et al. [33] evaluated S1-SM estimations at a 1 km grid scale, obtained using the change detection algorithm, against 5 cm in situ SM in several regions (Italy, Canada, USA, Denmark and Spain). They showed that the RMSE increases from 6.6 vol.% for the SM range between 5 and 20 vol.% to reach 15.2 vol.% for SM values between 30 vol.% and 55 vol.%. In a sensitivity analysis, they showed that, for VV polarization at a fixed low incidence angle (30°), the error in estimated S1 SM retrieval increases from dry to wet surfaces. This was found to be related to the fact that the standard error on the estimated SM has a positive linear correlation with the standard error on the backscattered SAR signal, which, itself, increases with the increase in the backscattered values. In the same context, Ma et al. [34] reported that the choice of the initial range of SM values before calibrating any data-driven model for SM estimation could have a direct effect on the retrieved SM values. They observed that considering a wide range of SM values for model calibration (between 5 vol.% and 50 vol.%) decreased the accuracy of SM retrieval in terms of both the correlation coefficient and RMSE. Conversely, a narrower soil moisture range between 15 vol.% and 45 vol.% yielded superior estimation results. A recent study by Arias et al. [35] evaluating S1 SM retrievals in wheat fields revealed that moisture content significantly impacted SM estimation accuracy. They noted higher errors in dry conditions in rain-fed fields compared to wetter conditions in irrigated fields. These findings align with our study, where SM estimations exhibited larger biases for dry conditions (SM less than 10 vol.%) compared to wetter conditions during irrigation (as observed in irrigated tomato fields). Moreover, extremely wet conditions (>35 vol.%) also showed lower accuracy in SM estimations compared to moderate SM conditions (between 10 and 30 vol.%).

In this study, our analysis revealed that the comparison between the S1-estimated soil moisture and the 10 cm in situ soil moisture was not always relevant and depends on several factors, such as the soil moisture conditions, the vegetation development and the S1 incidence angle. As previously discussed, the penetration of the S1 SAR signal in the soil layer can be challenging to quantify, and therefore the comparison between the S1 estimated SM and the common 10 cm SM measurements could be misleading. Notably, our observations indicated that, for very dry conditions (the case seen for tomato crop), the S1 SM extremely underestimated the 10 cm soil moisture. This was found to be due to the presence of topsoil slaking crust or a mulch, which led to a high difference between the 10 cm depth SM and the topsoil-measured SM values. Supporting this observation, Morrison et al. [36] highlighted in a laboratory-based study that anomalous soil moisture estimates can arise from the presence of subsurface features (such as the case of mulch). In their study, they concluded that the backscattering of the C-band SAR signal from the surface and subsurface is dependent on several factors, including soil moisture, soil

structure, incidence angle and the polarization of the SAR sensor. Similarly, a recent study by Ullmann et al. [16] explored the S1 backscatter time series variations in extremely arid areas and found a weak relationship between in situ soil moisture and S1 SAR intensities. Additionally, recent studies [37] showed that C-band soil moisture retrievals were of poor quality in arid environments due to subsurface scattering that may lead to large errors when estimating the SM by using the C-band backscattering values. Therefore, the integration of the soil texture and soil type as a factor in analyzing the S1 SM estimations' accuracy is crucial. However, in our study, limited variation in soil texture among the studied plots hindered us from obtaining significant results to compare the impact of soil texture and soil type variations on the S1 SM estimations. Integrating this factor into the analysis stands out as a critical aspect for future work.

For extremely wet conditions, the limitation in the S1-estimated SM is directly associated with the saturation and decrease in the S1 backscattered signal for very high soil moisture values. While the S1 backscattering coefficient could have a positive correlation with SM values, the S1 backscattered signal started to decrease when the SM increased beyond 35 vol.%. Deep in details, the radar signal for a given soil condition with SM close to 40 vol.% is similar to that for soil conditions with SM near 30 vol.%, since the radar signal stops increasing with the SM beyond an SM threshold of 30–35 vol.%. As a result, the estimation of the SM for these two soil conditions (with SM of 30 and 40 vol.%) will be similar and lower than 30 vol.%. This effect of decreased backscattering coefficients with extremely wet conditions was also validated in previous studies comparing the C-band modelled backscattering with in situ SM measurements and presented in the analysis performed in this study [38].

Various studies have highlighted the significant impact of the SAR incidence angle on the retrieved SM estimations. Baghdadi et al. [17], for instance, analyzed the sensitivity of the radar signal to soil moisture depending on the incidence angle. Their findings demonstrated that, specifically for bare soil in VV polarization at the C band, the sensitivity of the radar signal to SM decreases from 0.245 dB/vol.% for incidences between 21° and 25° to 0.079 dB/vol.% for incidences between 39° and 45° (it reaches an order of 0.232 dB/vol.% for incidences between 34° and 37°). This sensitivity analysis aligns with our study's validation, revealing that the optimal estimation of S1-based soil moisture occurred with lower incidence angles (<35°). Conversely, as the SAR incidence angle increased, the error in S1-based soil moisture estimations also increased.

4.3. Vegetation Effect on S1 SM Retrievals and Recommendation for End Users

For hydrological or agronomic purposes necessitating precise soil moisture data, this section provides a summary intended for end users, highlighting the reliability of S1-based soil moisture estimates across various crop types, including similar crops within the same family. A key focus of this study was evaluating the reliability of S1-derived soil moisture estimates throughout the growth cycle of vegetated plots. Table 3 outlines the primary limitations identified in S1 estimations related to vegetation development, as deduced from this investigation.

Table 3. Summary of the relevance of S1 SM estimates during the crop cycle of the studied crops and similar crops of the same family.

Crop Type	S1 SM Relevance	Reason for Limitation	Suitable NDVI Interval for SM Estimates
Tomato and similar aboveground vegetables	From beginning of the cycle until fruits' development	Presence of fruits increases S1 backscattering, causing a slight overestimation of SM	From 0 to 0.7
Wheat and similar straw cereals	From the beginning of the cycle until the gemination phase, and then after the heading phase	Wheat kernels attenuate the S1 backscattering, causing the loss of the soil contribution on the signal	NDVI between 0 and 0.6
Soybean and similar pea-family crops	From the beginning of the cycle until the pod's development	Bean pods increase the S1 backscattering, causing a high overestimation of SM	NDVI between 0 and 0.6

For tomato plants and similar aboveground vegetables crops, like peppers, eggplants, cucumbers and zucchini, the applicability of S1 estimates remains relevant from the initial stages of the crop cycle until the onset of fruit development, after which S1-derived soil moisture tends to overestimate the actual soil moisture. The results of our analysis revealed that, for such vegetable crops, the emergence of aboveground fruits, coupled with an increase in vegetation water content, results in increased S1 backscattering signals. This increase is primarily attributed to the geometry of the fruits, leading to a slight overestimation of soil moisture values by the S1 estimates. This effect was particularly noticeable in the tomato plot, where S1-estimated soil moisture values at 5 cm exceeded the soil moisture at 10 cm in depth—typically expected to be higher than the 5 cm soil moisture—following the development of fruits (as shown in Figures 6a and 10a). This phase of unreliable soil moisture estimates for these crops aligns with NDVI values typically exceeding 0.7.

For wheat crops, along with similar straw cereals, like barley and oat, as well as grasses exhibiting analogous geometrical and phenological traits to wheat, S1-based soil moisture estimates are reliable only from the early stages of the crop cycle until the heading phase (typically around March–April for winter wheat). This period corresponds to the growth phase characterized by an NDVI of less than 0.7. During the period between germination and heading phases in straw cereals, the vertical structure of wheat kernels significantly attenuates the S1 backscattering signal, resulting in minimal soil moisture contribution and, hence, inaccurate S1 soil moisture estimates. This diminished soil moisture contribution is evident in Figure 7a,b and Figure 10b. Post heading phase, when wheat kernels begin to dry, the S1 backscattering signal regains its sensitivity to soil moisture, rendering the S1 soil moisture estimates viable again. El Hajj et al. [18] showed that the sensitivity of the S1 signal to soil moisture diminishes as NDVI values for wheat crops increase. For NDVI values exceeding 0.7, the sensitivity of S1 to soil moisture sharply decreases, becoming negligible (in C-VV, sensitivity is 0.17 dB/vol.% for NDVI below 0.4, 0.15 dB/vol.% for NDVI between 0.4 and 0.7, and 0 dB/vol.% for NDVI higher than 0.7).

For soybean crops and related leguminous plants, like peas, lentils, chickpeas and fava beans, the reliability of S1 soil moisture estimates is limited to the early stages of the crop cycle until the elongated beans' pods start developing, typically corresponding to an NDVI range of about 0.6 to 0.7. During the growth phase when these pods emerge along the stems of the soybean, the S1 backscattering signal increases due to the geometric structure of the pods. This increase leads to a significant overestimation of in situ soil moisture values, as shown in Figure 9 for the soybean plot between July and October (for summer soybean). In such cases, the high magnitude of the S1 backscattered signal primarily represents the vegetation structure rather than the soil moisture values. The substantial overestimation of soil moisture persists from the appearance of the pods until the harvest of the soybean.

Finally, it was noticed from the provided analysis that S1 SM estimates do not always reflect the soil moisture values in the deep soil layers (example of 10 cm). Thus, users using

the S1 SM estimates in their applications must be aware that the retrieved information corresponds only to the surface soil moisture until 5 cm in depth, which cannot be representative of the deep soil moisture. Therefore, the use of S1 SM estimates as a source of soil moisture information for agronomical applications interested in deep soil moisture estimations (at 10 or 20 cm) could be risky. Hydrological applications, such as assessing runoff, infiltration rates or floods, relying on topsoil moisture estimations can still use the S1 SM estimates as a reliable source of information with a constraint on the developed vegetation cover during the peak of vegetation development. In addition, S1 SM estimations can still be significant for applications concerning irrigation detection and managements to optimize irrigation practices and monitor water stress [39–41]. Nevertheless, validating the S1 SM estimations requires performing in situ measurements limited to the first soil layer from 0 to 5 cm to have a consistent evaluation for the measured and estimated SM. The effect of the incidence angle on the SM retrieval could also not be neglected, as the results demonstrated that optimal SM estimations are found for a low incidence angle of the S1 signal. Thus, researchers making applications at a large scale, covering the whole S1 footprint, with an incidence angle usually ranging between 30° and 50°, should be aware of the estimations' accuracies as a function of the incidence angle over large study sites.

5. Conclusions

This study provided an assessment of the limitation of the S1-S2-derived soil moisture product (S^2MP) for estimating the soil moisture at the agricultural field scale over common cultivated crops, including wheat (straw cereal crops), tomato (aboveground vegetables), soybean (pea crops) and soil cover crops. Three key aspects were considered, namely the C-band penetration depth compared to conventional 10 cm in situ measurements, the vegetation cover development and the S1 incidence angle. A comparison of the estimated S1 SM and the generally performed in situ measurements at a 10 cm depth showed that the S1 SM is not always representative of the 10 cm SM and could underestimate the 10 cm SM, especially at dry conditions. This limitation was found to be most probably due to the difference between the SM values at the topsoil with a depth of a few cm (~5 cm) captured by the S1 sensor and the deeper SM values at 10 cm. The main recommendation for end users suggests that the use of S1-estimated SM remains reliable only for applications concerning surface soil moisture values. S1-estimated SM is less favored for applications requiring deeper soil moisture estimations. Concerning the vegetation development and its effect on the SM retrieval, the main results showed that, for studied crop types, as well as their corresponding crop family, the S1 SM estimates could be only valid for low and moderate vegetation cover with an NDVI less than 0.7. Where tomato (aboveground vegetables) and soybean (pea) showed overestimated SM values for developed vegetation cover with fruits' emergence, wheat (straw cereals) showed extremely underestimated SM for very well-developed vegetation cover. Thus, the recommendation for end users encouraged that the most suitable NDVI interval for reliable S1 SM estimates for these crops ranges between 0 and 0.7. Finally, the results suggested that S1 SM estimates are more favorable for low and medium radar incidence angles. Future work will concentrate on expanding the S^2MP accuracy analysis by considering other important factors that were not yet evaluated in this study, including the soil type, soil texture and other meteorological variables (precipitation, evapotranspiration, etc.).

Author Contributions: Conceptualization, H.B. and N.B.; data curation, H.B., N.B., P.N., R.N. and S.N.; formal analysis, H.B., N.B., P.N. and R.N.; methodology, H.B. and N.B.; software, H.B.; supervision, N.B., M.Z. and E.V.; validation, H.B. and N.B., M.Z. and E.V.; writing—original draft, H.B., N.B. and P.N.; writing—review and editing, P.N., R.N., S.N., M.Z. and E.V. All authors have read and agreed to the published version of the manuscript.

Funding: This research received funding from the POLYPHEME project of the TOSCA2023 program funded by the French Space Study Center (CNES) (grant number 24001897/id7689); the National Research Institute for Agriculture, Food and the Environment (INRAE); and in the framework of the

STEROPES project of the European Union's Horizon H2020 research and innovation European Joint Programme Cofund on Agricultural Soil Management (EJP-SOIL grant number 862695).

Data Availability Statement: Sentinel-1 data are available via the Copernicus open-access hub (https://scihub.copernicus.eu/dhus/#/home, accessed on 13 July 2023). Sentinel-2 data are available on the Theia French Land Data Center website (https://www.theia-land.fr/en/product/sentinel-2-surface-reflectance/, accessed on 13 July 2023).

Acknowledgments: The authors wish to thank the French Space Study Center (CNES, TOSCA 2023), and the MELICERTES project (ANR-22-PEAE-0010) of the French National Research Agency (France2030 and national PEPR "agroécologie et numérique" programmes). The authors would like to thank Pennelli Bruno (CREA) for providing SM data for the IT-LAZ Study area and Ialina Vinci (ARPAV Veneto) for providing SM data for the IT-VE Study area. The authors would like to also thank the European Space Agency (ESA) for providing the S1 images and the French Land Data Center (Theia) for providing the S2 images.

Conflicts of Interest: The authors declare no conflict of interest.

References

1. Massari, C.; Modanesi, S.; Dari, J.; Gruber, A.; De Lannoy, G.J.M.; Girotto, M.; Quintana-Seguí, P.; Le Page, M.; Jarlan, L.; Zribi, M.; et al. A Review of Irrigation Information Retrievals from Space and Their Utility for Users. *Remote Sens.* **2021**, *13*, 4112. [CrossRef]
2. Quast, R.; Wagner, W.; Bauer-Marschallinger, B.; Vreugdenhil, M. Soil Moisture Retrieval from Sentinel-1 Using a First-Order Radiative Transfer Model—A Case-Study over the Po-Valley. *Remote Sens. Environ.* **2023**, *295*, 113651. [CrossRef]
3. Bauer-Marschallinger, B.; Freeman, V.; Cao, S.; Paulik, C.; Schaufler, S.; Stachl, T.; Modanesi, S.; Massari, C.; Ciabatta, L.; Brocca, L.; et al. Toward Global Soil Moisture Monitoring with Sentinel-1: Harnessing Assets and Overcoming Obstacles. *IEEE Trans. Geosci. Remote Sens.* **2019**, *57*, 520–539. [CrossRef]
4. El Hajj, M.; Baghdadi, N.; Zribi, M.; Bazzi, H. Synergic Use of Sentinel-1 and Sentinel-2 Images for Operational Soil Moisture Mapping at High Spatial Resolution over Agricultural Areas. *Remote Sens.* **2017**, *9*, 1292. [CrossRef]
5. Entekhabi, D.; Njoku, E.G.; O'Neill, P.E.; Kellogg, K.H.; Crow, W.T.; Edelstein, W.N.; Entin, J.K.; Goodman, S.D.; Jackson, T.J.; Johnson, J.; et al. The Soil Moisture Active Passive (SMAP) Mission. *Proc. IEEE* **2010**, *98*, 704–716. [CrossRef]
6. Kerr, Y.H.; Waldteufel, P.; Wigneron, J.-P.; Martinuzzi, J.; Font, J.; Berger, M. Soil Moisture Retrieval from Space: The Soil Moisture and Ocean Salinity (SMOS) Mission. *IEEE Trans. Geosci. Remote Sens.* **2001**, *39*, 1729–1735. [CrossRef]
7. Wagner, W.; Hahn, S.; Kidd, R.; Melzer, T.; Bartalis, Z.; Hasenauer, S.; Figa-Saldana, J.; De Rosnay, P.; Jann, A.; Schneider, S.; et al. The ASCAT Soil Moisture Product: A Review of Its Specifications, Validation Results, and Emerging Applications. *Meteorol. Z.* **2013**, *22*, 5–33. [CrossRef]
8. Wigneron, J.-P.; Li, X.; Frappart, F.; Fan, L.; Al-Yaari, A.; De Lannoy, G.; Liu, X.; Wang, M.; Le Masson, E.; Moisy, C. SMOS-IC Data Record of Soil Moisture and L-VOD: Historical Development, Applications and Perspectives. *Remote Sens. Environ.* **2021**, *254*, 112238. [CrossRef]
9. Kornelsen, K.C.; Coulibaly, P. Advances in Soil Moisture Retrieval from Synthetic Aperture Radar and Hydrological Applications. *J. Hydrol.* **2013**, *476*, 460–489. [CrossRef]
10. Singh, A.; Gaurav, K. Deep Learning and Data Fusion to Estimate Surface Soil Moisture from Multi-Sensor Satellite Images. *Sci. Rep.* **2023**, *13*, 2251. [CrossRef]
11. Singh, S.K.; Prasad, R.; Srivastava, P.K.; Yadav, S.A.; Yadav, V.P.; Sharma, J. Incorporation of First-Order Backscattered Power in Water Cloud Model for Improving the Leaf Area Index and Soil Moisture Retrieval Using Dual-Polarized Sentinel-1 SAR Data. *Remote Sens. Environ.* **2023**, *296*, 113756. [CrossRef]
12. Das, N.N.; Entekhabi, D.; Dunbar, R.S.; Chaubell, M.J.; Colliander, A.; Yueh, S.; Jagdhuber, T.; Chen, F.; Crow, W.; O'Neill, P.E.; et al. The SMAP and Copernicus Sentinel 1A/B Microwave Active-Passive High Resolution Surface Soil Moisture Product. *Remote Sens. Environ.* **2019**, *233*, 111380. [CrossRef]
13. Bazzi, H.; Baghdadi, N.; El Hajj, M.; Zribi, M.; Belhouchette, H. A Comparison of Two Soil Moisture Products S^2MP and Copernicus-SSM Over Southern France. *IEEE J. Sel. Top. Appl. Earth Obs. Remote Sens.* **2019**, *12*, 3366–3375. [CrossRef]
14. Fan, J.; Han, Q.; Tan, S.; Li, J. Evaluation of Six Satellite-Based Soil Moisture Products Based on in Situ Measurements in Hunan Province, Central China. *Front. Environ. Sci.* **2022**, *10*, 829046. [CrossRef]
15. Escorihuela, M.J.; Quintana-Seguí, P. Comparison of Remote Sensing and Simulated Soil Moisture Datasets in Mediterranean Landscapes. *Remote Sens. Environ.* **2016**, *180*, 99–114. [CrossRef]
16. Ullmann, T.; Jagdhuber, T.; Hoffmeister, D.; May, S.M.; Baumhauer, R.; Bubenzer, O. Exploring Sentinel-1 Backscatter Time Series over the Atacama Desert (Chile) for Seasonal Dynamics of Surface Soil Moisture. *Remote Sens. Environ.* **2023**, *285*, 113413. [CrossRef]
17. Baghdadi, N.; Cerdan, O.; Zribi, M.; Auzet, V.; Darboux, F.; El Hajj, M.; Kheir, R.B. Operational Performance of Current Synthetic Aperture Radar Sensors in Mapping Soil Surface Characteristics in Agricultural Environments: Application to Hydrological and Erosion Modelling. *Hydrol. Process.* **2008**, *22*, 9–20. [CrossRef]

18. El Hajj, M.; Baghdadi, N.; Bazzi, H.; Zribi, M. Penetration Analysis of SAR Signals in the C and L Bands for Wheat, Maize, and Grasslands. *Remote Sens.* **2019**, *11*, 31. [CrossRef]
19. Gao, Q.; Zribi, M.; Escorihuela, M.; Baghdadi, N. Synergetic Use of Sentinel-1 and Sentinel-2 Data for Soil Moisture Mapping at 100 m Resolution. *Sensors* **2017**, *17*, 1966. [CrossRef]
20. Vanino, S.; Nino, P.; De Michele, C.; Falanga Bolognesi, S.; D'Urso, G.; Di Bene, C.; Pennelli, B.; Vuolo, F.; Farina, R.; Pulighe, G.; et al. Capability of Sentinel-2 Data for Estimating Maximum Evapotranspiration and Irrigation Requirements for Tomato Crop in Central Italy. *Remote Sens. Environ.* **2018**, *215*, 452–470. [CrossRef]
21. Stevanato, L.; Baroni, G.; Cohen, Y.; Fontana, C.L.; Gatto, S.; Lunardon, M.; Marinello, F.; Moretto, S.; Morselli, L. A Novel Cosmic-Ray Neutron Sensor for Soil Moisture Estimation over Large Areas. *Agriculture* **2019**, *9*, 202. [CrossRef]
22. Gianessi, S.; Polo, M.; Stevanato, L.; Lunardon, M.; Francke, T.; Oswald, S.; Ahmed, H.; Tolosa, A.; Weltin, G.; Dercon, G.; et al. Testing a Novel Sensor Design to Jointly Measure Cosmic-Ray Neutrons, Muons and Gamma Rays for Non-Invasive Soil Moisture Estimation. *Geosci. Instrum. Method. Data Syst. Discuss.* 2022; *in review*. [CrossRef]
23. El Hajj, M.; Baghdadi, N.; Zribi, M.; Rodríguez-Fernández, N.; Wigneron, J.; Al-Yaari, A.; Al Bitar, A.; Albergel, C.; Calvet, J.-C. Evaluation of SMOS, SMAP, ASCAT and Sentinel-1 Soil Moisture Products at Sites in Southwestern France. *Remote Sens.* **2018**, *10*, 569. [CrossRef]
24. Baghdadi, N.; El Hajj, M.; Zribi, M.; Bousbih, S. Calibration of the Water Cloud Model at C-Band for Winter Crop Fields and Grasslands. *Remote Sens.* **2017**, *9*, 969. [CrossRef]
25. Bazzi, H.; Baghdadi, N.; Charron, F.; Zribi, M. Comparative Analysis of the Sensitivity of SAR Data in C and L Bands for the Detection of Irrigation Events. *Remote Sens.* **2022**, *14*, 2312. [CrossRef]
26. Benninga, H.-J.F.; van der Velde, R.; Su, Z. Soil Moisture Content Retrieval over Meadows from Sentinel-1 and Sentinel-2 Data Using Physically Based Scattering Models. *Remote Sens. Environ.* **2022**, *280*, 113191. [CrossRef]
27. Ulaby, F.T.; Moore, R.K.; Fung, A.K. *Microwave Remote Sensing: Active and Passive. Volume 3—From Theory to Applications*; Artech House: London, UK, 1986.
28. Bruckler, L.; Witono, H.; Stengel, P. Near Surface Soil Moisture Estimation from Microwave Measurements. *Remote Sens. Environ.* **1988**, *26*, 101–121. [CrossRef]
29. Zhu, L.; Walker, J.P.; Ye, N.; Rüdiger, C. Roughness and Vegetation Change Detection: A Pre-Processing for Soil Moisture Retrieval from Multi-Temporal SAR Imagery. *Remote Sens. Environ.* **2019**, *225*, 93–106. [CrossRef]
30. Dong, L.; Baghdadi, N.; Ludwig, R. Validation of the AIEM Through Correlation Length Parameterization at Field Scale Using Radar Imagery in a Semi-Arid Environment. *IEEE Geosci. Remote Sens. Lett.* **2013**, *10*, 461–465. [CrossRef]
31. Grote, K.; Anger, C.; Kelly, B.; Hubbard, S.; Rubin, Y. Characterization of Soil Water Content Variability and Soil Texture Using GPR Groundwave Techniques. *J. Environ. Eng. Geophys.* **2010**, *15*, 93–110. [CrossRef]
32. Dabrowska-Zielinska, K.; Musial, J.; Malinska, A.; Budzynska, M.; Gurdak, R.; Kiryla, W.; Bartold, M.; Grzybowski, P. Soil Moisture in the Biebrza Wetlands Retrieved from Sentinel-1 Imagery. *Remote Sens.* **2018**, *10*, 1979. [CrossRef]
33. Balenzano, A.; Mattia, F.; Satalino, G.; Lovergine, F.P.; Palmisano, D.; Peng, J.; Marzahn, P.; Wegmüller, U.; Cartus, O.; Dąbrowska-Zielińska, K.; et al. Sentinel-1 Soil Moisture at 1 Km Resolution: A Validation Study. *Remote Sens. Environ.* **2021**, *263*, 112554. [CrossRef]
34. Ma, C.; Li, X.; McCabe, M.F. Retrieval of High-Resolution Soil Moisture through Combination of Sentinel-1 and Sentinel-2 Data. *Remote Sens.* **2020**, *12*, 2303. [CrossRef]
35. Arias, M.; Notarnicola, C.; Campo-Bescós, M.Á.; Arregui, L.M.; Álvarez-Mozos, J. Evaluation of Soil Moisture Estimation Techniques Based on Sentinel-1 Observations over Wheat Fields. *Agric. Water Manag.* **2023**, *287*, 108422. [CrossRef]
36. Morrison, K.; Wagner, W. Explaining Anomalies in SAR and Scatterometer Soil Moisture Retrievals from Dry Soils with Subsurface Scattering. *IEEE Trans. Geosci. Remote Sens.* **2020**, *58*, 2190–2197. [CrossRef]
37. Wagner, W.; Lindorfer, R.; Melzer, T.; Hahn, S.; Bauer-Marschallinger, B.; Morrison, K.; Calvet, J.-C.; Hobbs, S.; Quast, R.; Greimeister-Pfeil, I.; et al. Widespread Occurrence of Anomalous C-Band Backscatter Signals in Arid Environments Caused by Subsurface Scattering. *Remote Sens. Environ.* **2022**, *276*, 113025. [CrossRef]
38. Aubert, M.; Baghdadi, N.N.; Zribi, M.; Ose, K.; El Hajj, M.; Vaudour, E.; Gonzalez-Sosa, E. Toward an Operational Bare Soil Moisture Mapping Using TerraSAR-X Data Acquired Over Agricultural Areas. *IEEE J. Sel. Top. Appl. Earth Obs. Remote Sens.* **2013**, *6*, 900–916. [CrossRef]
39. Bazzi, H.; Baghdadi, N.; Najem, S.; Jaafar, H.; Le Page, M.; Zribi, M.; Faraslis, I.; Spiliotopoulos, M. Detecting Irrigation Events over Semi-Arid and Temperate Climatic Areas Using Sentinel-1 Data: Case of Several Summer Crops. *Agronomy* **2022**, *12*, 2725. [CrossRef]
40. Zappa, L.; Schlaffer, S.; Bauer-Marschallinger, B.; Nendel, C.; Zimmerman, B.; Dorigo, W. Detection and Quantification of Irrigation Water Amounts at 500 m Using Sentinel-1 Surface Soil Moisture. *Remote Sens.* **2021**, *13*, 1727. [CrossRef]
41. Modanesi, S.; Massari, C.; Bechtold, M.; Lievens, H.; Tarpanelli, A.; Brocca, L.; Zappa, L.; De Lannoy, G.J.M. Challenges and Benefits of Quantifying Irrigation through the Assimilation of Sentinel-1 Backscatter Observations into Noah-MP. *Hydrol. Earth Syst. Sci.* **2022**, *26*, 4685–4706. [CrossRef]